

Chirality of magnetic excitations in ferromagnetic SrRuO₃


K. Jenni,¹ S. Kunkemöller,¹ W. Schmidt², P. Steffens,³ A. A. Nugroho⁴, and M. Braden^{1,*}

¹*II. Physikalisches Institut, Universität zu Köln, Zùlpicher Str. 77, D-50937 Köln, Germany*

²*Forschungszentrum Jùlich GmbH, Jùlich Centre for Neutron Science at ILL, 38042 Grenoble, France*

³*Institut Laue Langevin, 71 avenue des Martyrs, 38000 Grenoble, France*

⁴*Faculty of Mathematics and Natural Science, Institut Teknologi Bandung, Jalan Ganesha 10, 40132 Bandung, Indonesia*

 (Received 27 January 2022; revised 23 March 2022; accepted 30 March 2022; published 16 May 2022)

Ferromagnetic SrRuO₃ was proposed as a candidate material to exhibit an inverted magnon chirality due to a strong impact of spin-orbit coupling and Weyl fermions. By polarized inelastic neutron scattering under magnetic fields we determine the chirality of the ferromagnetic zone-center excitation as a function of temperature. Well in the ferromagnetic phase the excitation is perfectly chiral with the usual (right-handed) sign and only when the spontaneous magnetization is almost completely suppressed the chirality of the zone center magnetic excitations is reduced but does not change sign.

DOI: [10.1103/PhysRevB.105.L180408](https://doi.org/10.1103/PhysRevB.105.L180408)

The topology of the Bloch states induced by spin-orbit coupling (SOC) causes exotic transport phenomena but the impact on the spin dynamics is much less explored. Onoda, Mischenko, and Nagaosa (OMN) deduced that under certain circumstances the chirality of the spin-wave excitation in a ferromagnet can become left handed [1]. The right handedness of spin quantum dynamics follows from the right-handed commutation relation between the components of the spin operator [2]. Considering the simple ferromagnetic Hamiltonian with exchange coupling $J > 0$ and easy-axis anisotropy $D > 0$, $\mathcal{H} = -\sum_{i,j} J\mathbf{S}_i\mathbf{S}_j - \sum_i DSS_i^z$, the time derivative of the spin operator is given by the commutation $\frac{dS_i^x}{dt} = \frac{1}{\hbar}[S_i^x, \mathcal{H}]$ yielding $\frac{dS_i^x}{dt} = \frac{1}{\hbar}DSS_i^y$ and $\frac{dS_i^y}{dt} = -\frac{1}{\hbar}DSS_i^x$, which is called right handedness. This precession of the spin around its average direction along z is clockwise in the x, y plane and is illustrated in Fig. 1. The chirality of the spin-wave excitation can be directly sensed with polarized inelastic neutron scattering (INS) experiments and very early studies on ferrites confirmed the chiral character of the magnon and the expected sign [3]. In the absence of SOC the neutron polarization channel can be deduced from the spin conservation requiring that the neutron spin flips from parallel to antiparallel to the magnetic guide field in a scattering process creating a magnon (neutron energy loss corresponding to a positive energy throughout this paper). Note that the ground state of the sample corresponds to $-S$ with respect to the guide field and that the annihilation of a magnon (neutron energy gain or negative energies) requires the opposite spin-flip process with antiparallel initial polarization. OMN argue that SOC and the induced Bloch-wave-function topology can yield a change of the handedness and compare this effect to the inversion of the handedness of propagating electromagnetic waves in the

special case of simultaneous electric and magnetic resonances, which yields a negative refraction index [4].

The impact of Bloch-wave-function topology and Weyl points on the magnetotransport properties such as the anomalous Hall effect is well established [5,6], but the role for the spin excitations has been elaborated only recently [1,7,8] and there are little experimental studies. Near the crossing of electronic bands due to the magnetic exchange splitting SOC can yield Weyl points, where magnetization and single-particle current are proportional to each other [7,8]. Therefore, the transverse conductivity σ_{xy} describing the anomalous Hall effect and the quantity C_ϕ^{xy} determining the chirality of the magnetic excitation [2] can be calculated in a similar way [1,7]. Because the chiral susceptibility and C_ϕ^{xy} involve the S^+ step-up operator and because, in the absence of SOC, orbital and spin degrees can be decomposed, C_ϕ^{xy} is always negative in this case, in accord with the usual right handedness of the spin-wave excitation. The mixing of spin and orbital degrees near Weyl points, however, allows processes with inverted and very small energy differences ΔE , which determine C_ϕ^{xy} due to the ΔE^{-2} weighting [1,2]. OMN formulate conditions for the occurrence of left-handed spin excitations induced by SOC [1]: Orbital moments must be small while spin-orbit interaction must remain important, majority and minority spins contribute both to the density of states at the Fermi level, and band degeneracies must occur near the Fermi level. These conditions seem to be fulfilled in SrRuO₃ [9–11].

SrRuO₃ is the perovskite member of the Ruddlesden-Popper series of ruthenates, it undergoes two structural phase transitions at 975 and 800 K into an orthorhombic phase (space group $Pnma$ with lattice constants $a \sim c \sim \sqrt{2}a_{\text{cub}}$, $b \sim 2a_{\text{cub}}$, $a_{\text{cub}} = 3.93 \text{ \AA}$) [9,12,13]. For simplicity, we will nevertheless use the pseudocubic lattice for indexing unless it is explicitly specified. Large single crystals can be grown by the floating-zone technique and exhibit the ferromagnetic transition at 165 K, a low temperature magnetization of $\sim 1.6\mu_B$ and a residual resistance ratio of up to 75 [14]. In

*braden@ph2.uni-koeln.de

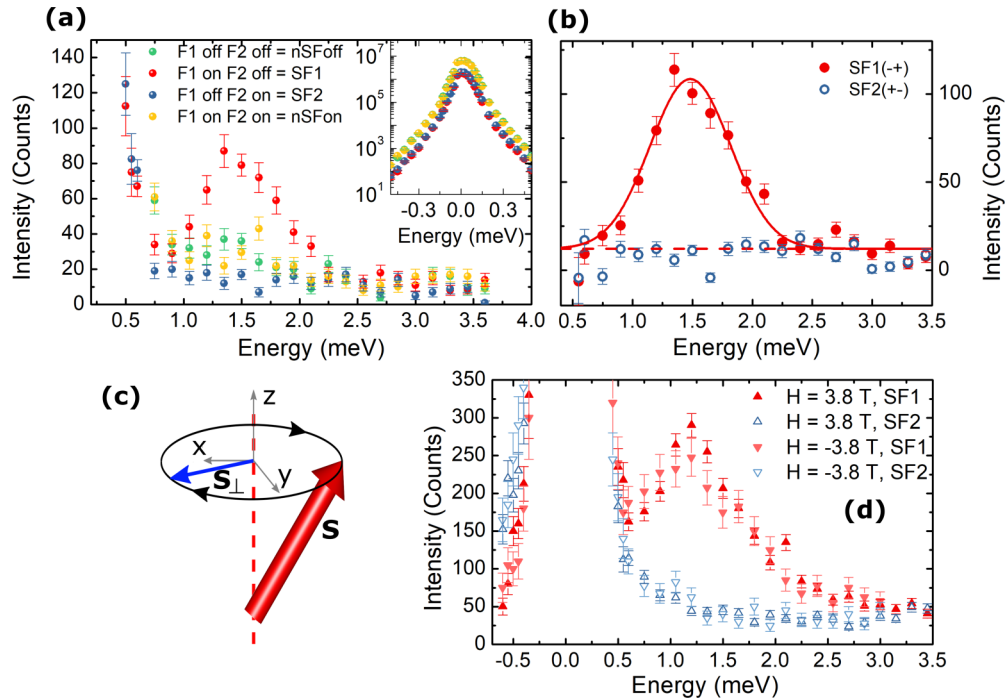


FIG. 1. (a) Raw data of constant \mathbf{Q} scans at $\mathbf{Q} = (0, 1, 1)$ and $T = 10$ K performed using a horizontal magnetic field of 3.8 T and different flipper configurations. The magnetic signal of the anisotropy gap in the inelastic response can be distinguished from nuclear contributions by the polarization analysis. The inset displays the elastic line for all four flipper configurations. (b) After correction, the magnon signal only appears in the corrected SF1 channel and is fitted with a Gaussian and constant background, while there is no signal visible in the SF2 channel. (c) The spin \mathbf{S} at site i in the excited state precesses around the quantization axis z clockwise. The perpendicular component \mathbf{S}_\perp follows the right-handed equation of motion derived in the text. (d) The influence of magnetic field direction on the magnon signal is studied by constant \mathbf{Q} scans for two different field directions at 160 K in both spin-flip channels (raw data).

spite of the considerable difference of magnetic and structural transition temperatures, it is possible to control the structural domains by applying large magnetic fields in the ferromagnetic phase yielding an almost perfect monodomain sample [15]. SrRuO_3 has attracted strong interest due to the close coupling of transport and magnetic properties [16,17], due to an invar effect occurring at the Curie temperature [18] and as a metallic and ferromagnetic electrode for functional perovskite materials [11]. Furthermore, the ferromagnetism of SrRuO_3 inspired a superconducting pairing mechanism for Sr_2RuO_4 based on ferromagnetic spin excitations [19,20], but the role of quasiferromagnetic fluctuations in the unconventional superconductivity remains matter of controversy [21]. In SrRuO_3 states at the Fermi level mainly stem from the Ru $4d$ orbitals, for which strong SOC can be assumed, but there is hybridization with the oxygen p levels so that about one third of the total ferromagnetic magnetization resides on the oxygen sites [22]. The experimental and calculated spin density distributions indicate an almost equal occupation of t_{2g} orbitals [22], and both spin states contribute to the density of states at the Fermi levels with minority spins dominating [23]. Density functional calculations and x-ray magnetic circular dichroism measurements find only a tiny orbital moment in SrRuO_3 , about a few percent of the spin contribution [22,24,25], but nevertheless the magnetic anisotropy is sizable: The gap of magnon dispersion amounts to about 1 meV [8] in agreement with optical measurements [26] and with the anisotropy extending up to ~ 10 T in magnetization measurements [14,15,27,28]. The easy axis of SrRuO_3 is the

orthorhombic c axis, which is a pseudocubic $[0,1,1]$ direction [15].

The anomalous Hall effect in SrRuO_3 has been intensively studied because it exhibits a sign change as a function of temperature [6–8,11,29–31]. By now there seems to be consensus that the anomalous Hall effect arises from the topology of the Bloch wave functions in the magnetically ordered state or more precisely from the Berry phase generated by Weyl points [6,7], which DFT calculations find to appear close to the Fermi level [32]. Comprehensive studies of the magnetotransport properties further corroborate the dominant role of the Weyl points [33]. The comparison of the temperature dependence of the magnon dispersion parameters, gap and stiffness, with that of the anomalous Hall effect indicates that the Weyl points also cause the renormalization of the spin-wave dispersion [7,8]. Here, single-crystal inelastic neutron scattering turned out to be decisive [8].

For the INS experiments on IN12 at ILL [34] we used a mounting of six large crystals with a total mass of about 3 g in the $[1,0,0]/[0,1,1]$ scattering plane similar to the previous unpolarized experiment [8]; detailed characterization of the crystals can be found in Refs. [14,15,22]. The neutron beam is polarized by a transmission polarizing cavity in front of the monochromator [34], which transmits neutrons with a polarization antiparallel to the guide field. In combination with two Mezei-flippers and a Heusler analyzer all four spin-flip (SF) channels can be measured. The here-used Heusler analyzer consists of Cu_2MnAl single crystals, which also transmit the polarization antiparallel to the

guide field. Without an active spin flipper this setup measures therefore the antiparallel nonspin-flip (nSF) channel $I^{\downarrow\downarrow}$. A large field of mostly 3.8 T (maximum value of horizontal magnet 134OXHV38 at ILL) was applied along [011] to enable neutron polarization analysis parallel to \mathbf{Q} . In the polarized neutron experiments we deal with different coordinate systems of the crystal lattice and of the polarization analysis that are illustrated in the Supplemental Material [35]. The INS data are available in Refs. [36,37].

By cooling the crystals in a field of 3 T we can imply a homogeneous magnetic state, see above, and partially compensate the intrinsic stray fields of the crystal assembly. But even with 3.8 T there is a clear reduction of the polarization performance when entering the ferromagnetic phase. Furthermore, the high external field affects the efficiency of the flipper on k_f even though the flipper currents were optimized as a function of the angle between the magnetic field and k_f . Flipping ratios were determined by analyzing the attenuated direct beam intensity and by measurements of Bragg peaks. Well above the ferromagnetic order we find a ratio of 24, which, however, is strongly reduced to 3.5 at 10 K. The high flipping ratio in the paramagnetic state is only obtained for flipper 1 that is situated far away from the horizontal magnet, while for flipper 2 the ratio is reduced to ≈ 14 . The raw polarized data were corrected for finite polarization and reduced flipper efficiency as described in the Supplemental Material [35]. I_{++} , I_{+-} , I_{-+} , and I_{--} denote the four polarization channels with + indicating flipper off (polarization antiparallel to guide fields), – flipper on, first index incoming and second outgoing beam.

Figures 1(a) and 1(b) present the polarized INS data for the uncorrected four channels and for the two corrected SF channels at 10 K, respectively. In this and following Figures the data are normalized to a monitor counting of 600.000, which roughly corresponds to 5 minutes counting time. We scan the positive transferred energy corresponding to magnon or phonon creation processes at constant $\mathbf{Q} = (0,1,1)$. With the direction of neutron polarization analysis fixed to parallel $\mathbf{Q} = (0,1,1)$ all magnetic scattering appears in the SF channels while nuclear and phonon scattering appears in the nSF channels. See the Supplemental Material [35] for further illustration of the geometrical conditions. The ordered magnetic moment is parallel to \mathbf{Q} and thus does not contribute to the scattering. The elastic Bragg signal shown in the inset of Fig. 1(a) thus stems entirely from the nuclear structure, and the sizable signal in the SF channels stems from the reduced polarization deep in the ferromagnetic phase. Both nSF channels exhibit significant intensity above the elastic line that can be attributed to phonon scattering. The usual correction for finite neutron polarization cannot treat the specific problem of our measurement with large horizontal fields. The efficiency of flipper 2 is strongly reduced but this applies only to the configuration when it is switched on. As described in the Supplemental Material [35] one has to separately correct for the finite polarization and for the reduced flipping in the second flipper. Both correction parameters can be independently determined. In the corrected SF channels separated in panel (b) there is a strong signal in $I_{-+} = \text{SF1}$ while $I_{+-} = \text{SF2}$ stays even below the nSF channels. I_{-+} corresponds to the configuration with incoming neutron polarization parallel to

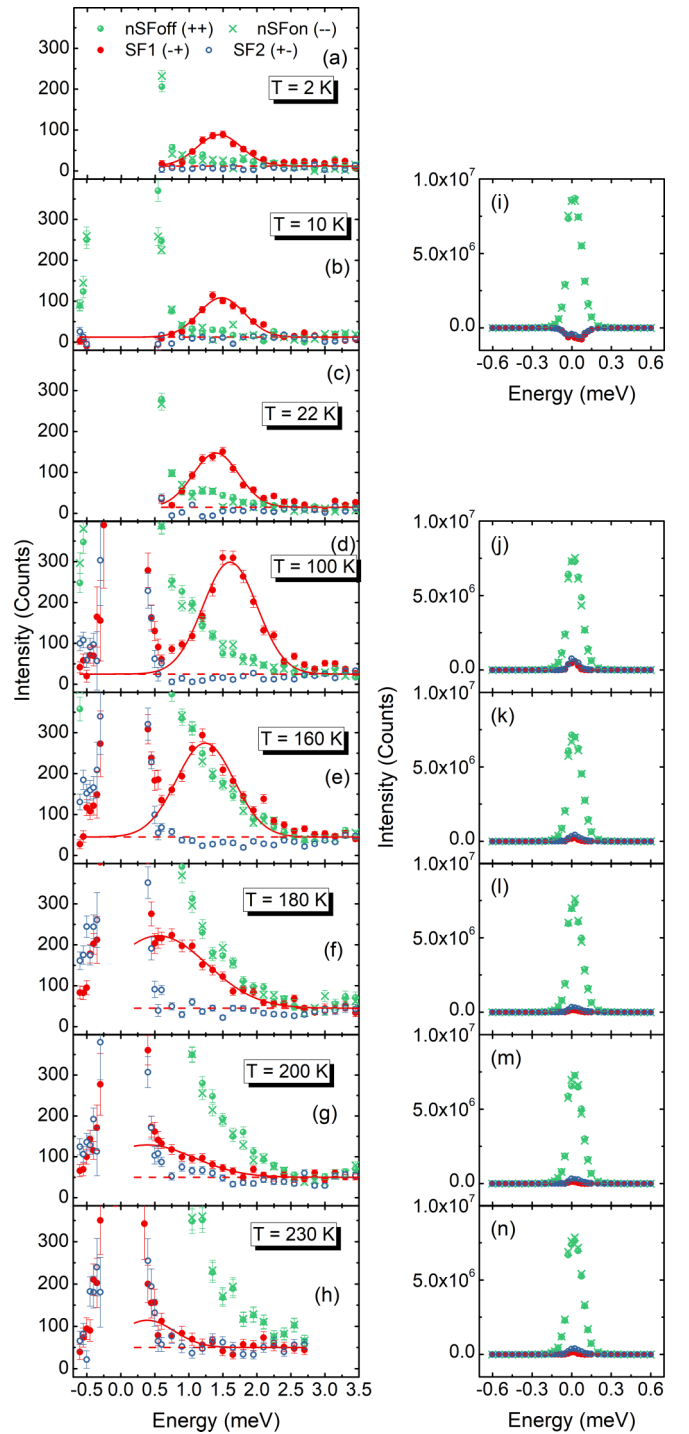


FIG. 2. Comparison of all four polarization channels nSFoff, nSFon, SF1, SF2 for various temperatures after applying the correction for finite polarization and flipper efficiency described in the Supplemental Material [35]. [(a)–(h)] The magnon signal in SF1 is fitted with a Gaussian and a constant background. [(i)–(n)] Corrected data around the elastic line. Note that the correction of data can lead to negative intensities, which can be only represented in a linear scale.

the sample magnetization that is enforced by the external field. Therefore, these data immediately show that the zone-center ferromagnetic excitations in SrRuO₃ exhibit the right-handed chirality. At first view it may astonish that the uncorrected data

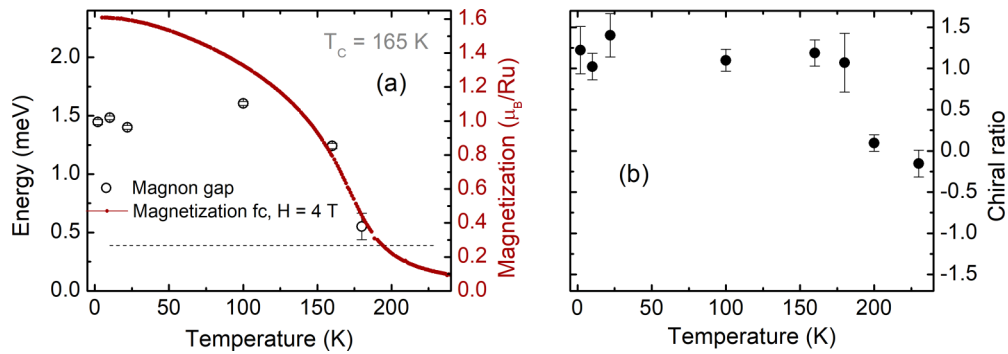


FIG. 3. Temperature dependence of the magnon gap and the chirality of the magnon: (a) The magnon gap as peak position of the fits of the corrected data in Fig. 2 (black circles) is compared to the field-cooled magnetization at 4 T with field parallel to $[0,1,1]$ direction (red dots). The dashed line designates the finite energy induced by Zeeman splitting [38]. (b) The chiral ratio as the normalized difference of both spin flip channels represents the chiral part of the magnetic scattering and exhibits no pronounced temperature dependence in the ferromagnetic phase but drops above ~ 200 K. The chiral ratio is based on corrected data.

yield such a clear statement even though the flipping ratio is rather poor. However, the chiral mode itself enhances the neutron polarization; one could even obtain this information without an incoming polarization (or without analyzing the final polarization) in a half-polarized mode. The clear balance of the SF intensities visible in Fig. 1(b) documents a perfect right-handed chirality.

The peak energy of the zone-center magnon in the scans at finite fields is higher than the results reported at zero field [8] due to the Zeeman energy added [38]. In Fig. 1(d) we compare similar scans taken at 160 K for positive and negative magnetic fields. In both cases the magnon excitation essentially appears in the SF1 channel corresponding to the incoming polarization being parallel to the magnetic field as it is expected. Note that in these cases we keep \mathbf{Q} identical but invert both the sample magnetization and the polarization direction so that the right-handed chirality appears in the same channel. However, the data at 160 K indicate some scattering in the SF2 channel whose analysis requires a correction of the finite polarization and efficiency of flipper 2, see Supplemental Material [35]. We also studied the chirality at $\mathbf{Q} = (0,0.95,0.95)$ and $(0,1.1,1.1)$ where all magnon scattering is again found in the SF1 I^{-+} channel and thus exhibits perfect right-handed chirality.

The corrected energy scan data for various temperatures are shown in Fig. 2. At 2, 10, and 22 K we only scanned the positive energy transfer and all magnon intensity appears in the SF1 channel indicating right handedness. At 100 and 160 K the data quality improves because the enhanced Bose factor implies larger signals. Furthermore, the intensity ratio of SF1 and SF2 is inverted at the negative energy transfer of ~ -0.5 meV corresponding to annihilation of excitations. The scans do not cover the full range of the magnon at negative energies, but only reach the tail of the excitation. The inverted ratio with SF2 > SF1 perfectly agrees with a right-handed excitation as it is discussed in the introduction. The magnon gap is traced as a function of temperature in Fig. 3(a), where it is compared to the magnetization measured at a field of 4 T. At this magnetic field the ferromagnetic transition is smeared out, as there is no longer a sharp phase transition associated with spontaneous symmetry breaking. The magnon gap clearly passes through a maximum value

around 100 K similar to the zero-field experiments [7,8]. This anomalous hardening upon heating is one of the impacts of the Weyl points on the spin dynamics. The chiral ratio CR of the scattering can be defined by:

$$\text{CR} = \frac{I_x^{\uparrow\downarrow} - I_x^{\downarrow\uparrow}}{I_x^{\uparrow\downarrow} + I_x^{\downarrow\uparrow}} = \frac{I_x^{-+} - I_x^{+-}}{I_x^{-+} + I_x^{+-}}$$

and is shown in Fig. 3(b). Well in the ferromagnetic ordered state we find a value of +1 indicating a perfect right-handed chirality.

At a temperature of 180 K the magnetization is already strongly reduced, which is reflected by the strong drop of both the magnon gap and intensity. This temperature lies above the inflection point of the temperature dependent magnetization curve obtained at 4 T. The description by a Gaussian is unsatisfying at 180 K and higher temperatures but serves as a guide to the eye. However, the magnon chirality still indicates a nearly ideal right handedness at 180 K. In contrast, the chiral ratio vanishes at 200 and 230 K indicating a qualitative change in the character of the magnetic excitations. At these two temperatures the spontaneous part of the magnetization is almost fully suppressed and the inelastic response at the ferromagnetic zone center should be considered as critical or paramagnon scattering under the impact of a finite field. Note, that the unpolarized INS experiments at higher energies revealed clear signatures of magnetic modes persisting well above the Curie temperature [8], which agree with the persistence of band energy splitting observed in ARPES experiments [39]. In contrast the magnon gap is more strongly coupled with long-range ordering and gets rapidly suppressed towards the Zeeman splitting at the finite field (indicated by the dashed line in Fig. 3). It is unambiguous that there still is low-energy magnetic scattering at these temperatures. In particular the SF2 data at 200 and 230 K are stronger than those at 180 K.

At the reduced magnetic field of 1 T the neutron polarization could only be maintained above 160 K, and Fig. 4 presents data taken at this temperature. Also at this reduced field and this temperature slightly below the ferromagnetic transition the magnon excitation exhibits a full right-handed character, but the 1 T data at 180 K and 200 K again indicate

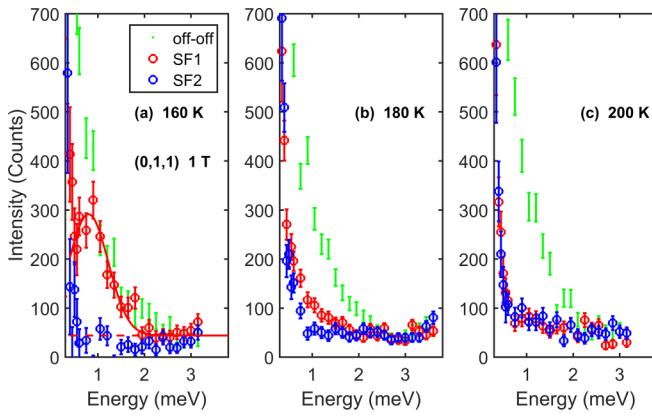


FIG. 4. At a magnetic field of 1 T polarized INS experiments were only possible above $T = 160$ K. At this temperature the magnon gap is reduced due to the smaller Zeeman term but the excitation still exhibits a nearly perfect right-handed character, panel (a). Similar to the data at 3.8 T further enhancement of the temperature, panels (b) and (c), leads to an intensity enhancement in channel SF2, which results in a magnetic signal at 200 K that is equally distributed in the two spin-flip channels.

the enhancement of inelastic scattering in the SF2 channel. At 200 K there is no significant intensity difference between the two channels. At both fields the magnetic response loses its chiral character above the onset of spontaneous magnetization. One can however not decide, whether this additional SF2 scattering arises from left-handed excitations, because nonchiral, for example uniaxial, magnetic excitations will also yield such a response. The question whether left-handed magnons do appear close to the suppression of the ferromagnetic ordering and at smaller fields requires further theoretical and experimental studies.

The perfect right-handed chirality seems to disagree with the strong effects the Bloch function topology implies on the temperature dependence of the magnon stiffness and gap in SrRuO_3 [7,8]. Both quantities get renormalized by the same correction factor. While low-temperature softening of stiffness and gap is unambiguously anomalous, the precise estimation of the normal behavior of these quantities is less obvious. In Refs. [7,8] the magnetization data was taken as a measure of the bare temperature dependence, which in view of the recently reported weak temperature dependence of the band energy splitting [39] may overestimate the renormalization.

In conclusion we have analyzed the chirality of the magnetic excitation at the ferromagnetic zone center in SrRuO_3 following the proposal that this material can exhibit an inverted handedness due to strong SOC. However, the polarized INS experiments find a perfect chirality with the sign predicted by the standard commutation rules of the spin components. The Berry phase implied by the topology of the Bloch functions seems insufficient to invert the handedness of the magnetic excitations at least well in the ferromagnetic state of SrRuO_3 . This finding persists upon heating to a temperature where the spontaneous magnetization is considerably weakened (above the inflection point of magnetization). Only at even higher temperatures the chirality of the low-energy zone-center magnetic excitations is lost, which however cannot be taken as evidence for left-handed excitations.

We wish to thank A. Rosch for stimulating discussions. This work was funded by the Deutsche Forschungsgemeinschaft (DFG, German Research Foundation) Project No. 277146847 - CRC 1238, Projects A02 and B04.

- [1] M. Onoda, A. S. Mishchenko, and N. Nagaosa, Left-handed spin wave excitation in ferromagnet, *J. Phys. Soc. Jpn.* **77**, 013702 (2008).
- [2] The commutation rules for a spin operator in units of \hbar are $[S^\alpha, S^\beta] = i\epsilon^{\alpha\beta\gamma}S^\gamma$ with α, β, γ the spatial coordinate indices and $\epsilon^{\alpha\beta\gamma}$ the Levi-Civita symbol. The magnon handedness is determined by $C_\Phi^{xy} = \frac{1}{2V} \sum_{m,m',k} \frac{f(\epsilon_{m'k}) - f(\epsilon_{mk})}{(\epsilon_{m'k} - \epsilon_{mk})^2} \cdot |\langle mk|S^+|m'k\rangle|^2$, with m, m' the band and spin indices, $\epsilon_{m'k}$ the energy, and f the Fermi function.
- [3] R. M. Moon, T. Riste, and W. C. Koehler, Polarization analysis of thermal-neutron scattering, *Phys. Rev.* **181**, 920 (1969).
- [4] S. A. Ramakrishna, Physics of negative refractive index materials, *Rep. Prog. Phys.* **68**, 449 (2005).
- [5] N. Nagaosa, J. Sinova, S. Onoda, A. H. MacDonald, and N. P. Ong, Anomalous Hall effect, *Rev. Mod. Phys.* **82**, 1539 (2010).
- [6] Z. Fang, N. Nagaosa, K. S. Takahashi, A. Asamitsu, R. Mathieu, T. Ogasawara, H. Yamada, M. Kawasaki, Y. Tokura, and K. Terakura, The anomalous Hall effect and magnetic monopoles in momentum space, *Science* **302**, 92 (2003).
- [7] S. Itoh, Y. Endoh, T. Yokoo, S. Ibuka, J.-G. Park, Y. Kaneko, K. S. Takahashi, Y. Tokura, and N. Nagaosa, Weyl fermions and spin dynamics of metallic ferromagnet SrRuO_3 , *Nat. Commun.* **7**, 11788 (2016).
- [8] K. Jenni, S. Kunkemöller, D. Brüning, T. Lorenz, Y. Sidis, A. Schneidewind, A. A. Nugroho, A. Rosch, D. I. Khomskii, and M. Braden, Interplay of Electronic and Spin Degrees in Ferromagnetic SrRuO_3 : Anomalous Softening of the Magnon Gap and Stiffness, *Phys. Rev. Lett.* **123**, 017202 (2019).
- [9] J. J. Randall and R. Ward, The preparation of some ternary oxides of the platinum metals, *J. Am. Chem. Soc.* **81**, 2629 (1959).
- [10] A. Callaghan, C. W. Moeller, and R. Ward, Magnetic interactions in ternary ruthenium oxides, *Inorg. Chem.* **5**, 1572 (1966).
- [11] G. Koster, L. Klein, W. Siemons, G. Rijnders, J. S. Dodge, C.-B. Eom, D. H. A. Blank, and M. R. Beasley, Structure, physical properties, and applications of SrRuO_3 thin films, *Rev. Mod. Phys.* **84**, 253 (2012).
- [12] C. W. Jones, P. D. Battle, P. Lightfoot, and W. T. A. Harrison, The structure of SrRuO_3 by time-of-flight neutron powder diffraction, *Acta Crystallogr. Sect. C: Cryst. Struct. Commun.* **45**, 365 (1989).
- [13] B. Chakoumakos, S. Nagler, S. Misture, and H. Christen, High-temperature structural behavior of SrRuO_3 , *Physica B: Condens. Matter* **241-243**, 358 (1997).
- [14] S. Kunkemöller, F. Sauer, A. A. Nugroho, and M. Braden, Magnetic anisotropy of large floating-zone-grown

- single-crystals of SrRuO₃, *Cryst. Res. Technol.* **51**, 299 (2016).
- [15] S. Kunkemöller, D. Brüning, A. Stunault, A. A. Nugroho, T. Lorenz, and M. Braden, Magnetic shape-memory effect in SrRuO₃, *Phys. Rev. B* **96**, 220406(R) (2017).
- [16] P. B. Allen, H. Berger, O. Chauvet, L. Forro, T. Jarlborg, A. Junod, B. Revaz, and G. Santi, Transport properties, thermodynamic properties, and electronic structure of SrRuO₃, *Phys. Rev. B* **53**, 4393 (1996).
- [17] L. Klein, J. S. Dodge, C. H. Ahn, G. J. Snyder, T. H. Geballe, M. R. Beasley, and A. Kapitulnik, Anomalous Spin Scattering Effects in the Badly Metallic Itinerant Ferromagnet SrRuO₃, *Phys. Rev. Lett.* **77**, 2774 (1996).
- [18] T. Kiyama, K. Yoshimura, K. Kosuge, Y. Ikeda, and Y. Bando, Invar effect of SrRuO₃: Itinerant electron magnetism of Ru 4d electrons, *Phys. Rev. B* **54**, R756 (1996).
- [19] T. Rice and M. Sigrist, Sr₂RuO₄: An electronic analogue of ³He? *J. Phys.: Condens. Matter* **7**, L643 (1995).
- [20] G. Baskaran, Why is Sr₂RuO₄ not a high *T_c* superconductor? Electron correlation, Hund's coupling and p-wave instability, *Physica B: Condens. Matter* **223-224**, 490 (1996).
- [21] P. Steffens, Y. Sidis, J. Kulda, Z. Q. Mao, Y. Maeno, I. I. Mazin, and M. Braden, Spin Fluctuations in Sr₂RuO₄ from Polarized Neutron Scattering: Implications for Superconductivity, *Phys. Rev. Lett.* **122**, 047004 (2019).
- [22] S. Kunkemöller, K. Jenni, D. Gorkov, A. Stunault, S. Streltsov, and M. Braden, Magnetization density distribution in the metallic ferromagnet SrRuO₃ determined by polarized neutron diffraction, *Phys. Rev. B* **100**, 054413 (2019).
- [23] D. C. Worledge and T. H. Geballe, Negative Spin-Polarization of SrRuO₃, *Phys. Rev. Lett.* **85**, 5182 (2000).
- [24] S. Agrestini, Z. Hu, C.-Y. Kuo, M. W. Haverkort, K.-T. Ko, N. Hollmann, Q. Liu, E. Pellegrin, M. Valvidares, J. Herrero-Martin, P. Gargiani, P. Gegenwart, M. Schneider, S. Esser, A. Tanaka, A. C. Komarek, and L. H. Tjeng, Electronic and spin states of SrRuO₃ thin films: An x-ray magnetic circular dichroism study, *Phys. Rev. B* **91**, 075127 (2015).
- [25] J. Okamoto, T. Okane, Y. Saitoh, K. Terai, S.-I. Fujimori, Y. Muramatsu, K. Yoshii, K. Mamiya, T. Koide, A. Fujimori, Z. Fang, Y. Takeda, and M. Takano, Soft x-ray magnetic circular dichroism study of Ca_{1-x}Sr_xRuO₃ across the ferromagnetic quantum phase transition, *Phys. Rev. B* **76**, 184441 (2007).
- [26] M. C. Langner, C. L. S. Kantner, Y. H. Chu, L. M. Martin, P. Yu, J. Seidel, R. Ramesh, and J. Orenstein, Observation of Ferromagnetic Resonance in SrRuO₃ by the Time-Resolved Magneto-Optical Kerr Effect, *Phys. Rev. Lett.* **102**, 177601 (2009).
- [27] A. Kanbayasi, Magnetic properties of SrRuO₃ single crystals, *J. Phys. Soc. Jpn.* **41**, 1876 (1976).
- [28] G. Cao, S. McCall, M. Shepard, J. E. Crow, and R. P. Guertin, Thermal, magnetic, and transport properties of single-crystal Sr_{1-x}Ca_xRuO₃, *Phys. Rev. B* **56**, 321 (1997).
- [29] M. Izumi, K. Nakazawa, Y. Bando, Y. Yoneda, and H. Terauchi, Magnetotransport of SrRuO₃ thin film on SrTiO₃ (001), *J. Phys. Soc. Jpn.* **66**, 3893 (1997).
- [30] Y. Kats, I. Genish, L. Klein, J. W. Reiner, and M. R. Beasley, Testing the Berry phase model for extraordinary Hall effect in SrRuO₃, *Phys. Rev. B* **70**, 180407(R) (2004).
- [31] N. Haham, Y. Shperber, M. Schultz, N. Naftalis, E. Shimshoni, J. W. Reiner, and L. Klein, Scaling of the anomalous Hall effect in SrRuO₃, *Phys. Rev. B* **84**, 174439 (2011).
- [32] Y. Chen, D. L. Bergman, and A. A. Burkov, Weyl fermions and the anomalous Hall effect in metallic ferromagnets, *Phys. Rev. B* **88**, 125110 (2013).
- [33] K. Takiguchi, Y. K. Wakabayashi, H. Irie, Y. Krockenberger, T. Otsuka, H. Sawada, S. A. Nikolaev, H. Das, M. Tanaka, Y. Taniyasu, and H. Yamamoto, Quantum transport evidence of Weyl fermions in an epitaxial ferromagnetic oxide, *Nat. Commun.* **11**, 4969 (2020).
- [34] K. Schmalzl, W. Schmidt, S. Raymond, H. Feilbach, C. Mounier, B. Vettard, and T. Brückel, The upgrade of the cold neutron three-axis spectrometer IN12 at the ILL, *Nucl. Instrum. Methods Phys. Res., Sect. A* **819**, 89 (2016).
- [35] See Supplemental Material at <http://link.aps.org/supplemental/10.1103/PhysRevB.105.L180408> for a detailed description of the polarization correction and the geometrical conditions of the experiment.
- [36] K. Jenni, M. Braden, S. Kunkemöller, and P. Steffens, (2018), left-handed magnons in the metallic ferromagnet SrRuO₃. Institut Laue-Langevin (ILL), doi:10.5291/ILL-DATA.4-01-1563.
- [37] K. Jenni, M. Braden, W. Schmidt, and P. Steffens, (2019), impact of spin-orbit coupling in the metallic ferromagnet SrRuO₃. Institut Laue-Langevin (ILL), doi:10.5291/ILL-DATA.4-01-1631.
- [38] INS experiments on PANDA yield a linear increase of the magnon gap with 0.103 meV/T.
- [39] S. Hahn, B. Sohn, M. Kim, J. R. Kim, S. Huh, Y. Kim, W. Kyung, M. Kim, D. Kim, Y. Kim, T. W. Noh, J. H. Shim, and C. Kim, Observation of Spin-Dependent Dual Ferromagnetism in Perovskite Ruthenates, *Phys. Rev. Lett.* **127**, 256401 (2021).